Monthly Notices
of the
ROYAL ASTRONOMICAL SOCIETY

Mon. Not. R. Astron. Soc. **412,** 1331–1340 (2011) doi:10.1111/j.1365-2966.2010.18017.x

Tidal excitations of oscillation modes in compact white dwarf binaries – I. Linear theory

Jim Fuller★ and Dong Lai★

Center for Space Research, Department of Astronomy, Cornell University, Ithaca, NY 14853, USA

Accepted 2010 November 5. Received 2010 November 4; in original form 2010 September 16

ABSTRACT

We study the tidal excitation of gravity modes (g-modes) in compact white dwarf binary systems with periods ranging from minutes to hours. As the orbit of the system decays via gravitational radiation, the orbital frequency increases and sweeps through a series of resonances with the g-modes of the white dwarf. At each resonance, the tidal force excites the g-mode to a relatively large amplitude, transferring the orbital energy to the stellar oscillation. We calculate the eigenfrequencies of g-modes and their coupling coefficients with the tidal field for realistic non-rotating white dwarf models. Using these mode properties, we numerically compute the excited mode amplitude in the linear approximation as the orbit passes though the resonance, including the back reaction of the mode on the orbit. We also derive analytical estimates for the mode amplitude and the duration of the resonance, which accurately reproduce our numerical results for most binary parameters. We find that the g-modes can be excited to a dimensionless (mass-weighted) amplitude up to 0.1, with the mode energy approaching 10^{-3} of the gravitational binding energy of the star. Therefore the low-frequency ($\lesssim 10^{-2}$ Hz) gravitational waveforms produced by the binaries, detectable by *LISA*, are strongly affected by the tidal resonances. Our results also suggest that thousands of years prior to the binary merger, the white dwarf may be heated up significantly by tidal interactions. However, more study is needed since the physical amplitudes of the excited oscillation modes become highly non-linear in the outer layer of the star, which can reduce the mode amplitude attained by tidal excitation.

Key words: binaries: close – stars: interiors – stars: kinematics and dynamics – stars: oscillations – white dwarfs.

1 INTRODUCTION

It is well known that non-radial gravity modes (g-modes) are responsible for the luminosity variations observed in some isolated white dwarfs (called ZZ Ceti stars) in the instability strip. These g-modes are thought to be excited by a convective driving mechanism operating in the shallow surface convection zone of the star (see Brickhill 1983; Goldreich & Wu 1999; Wu & Goldreich 1999).

In this paper we study the tidal excitation of g-modes in compact binary systems containing a white dwarf (WD) and another compact object (white dwarf, neutron star or black hole). The Galaxy is populated with $\sim 10^8$ WD–WD binaries and several 10^6 of double WD–NS binaries [Nelemans et al. (2001); see also Nelemans (2009) and references therein]. A sizeable fraction of these binaries are compact enough so that the binary orbit will decay within a Hubble time to initiate mass transfer or a binary merger. Depending on the details of the mass transfer process (including the response of the WD to mass transfer), these ultra-compact binaries (with orbital period less than an hour) may survive mass transfer for a long time or merge shortly after mass transfer begins. A number of ultra-compact interacting WD–WD binary systems have already been observed [including RX J0806.3+1527 (period 5.4 min) and V407 Vul (period 9.5 min); see Strohmayer 2005 and Ramsay et al. 2005]. Recent surveys (e.g. SDSS) have also begun to uncover non-interacting compact WD binaries (e.g. Badenes et al. 2009; Kilic et al. 2009; Mullally et al. 2009; Kulkarni & van Kerkwijk 2010; Marsh et al. 2010; Steinfadt et al. 2010). Depending on the total mass, the systems may evolve into Type Ia supernovae (for high mass), or become AM CVn binaries or R CrB stars (for low mass). Many of these WD binaries are detectable in gravitational waves (GW) by the *Laser Interferometer Space Antenna (LISA*; Nelemans 2009).

In this paper we consider resonant tidal interaction in WD binaries that are not undergoing mass transfer. This means that the binary separation D is greater than $D_{\rm min}$, the orbital radius at which dynamical merger or mass transfer occurs, i.e.

$$D \gtrsim D_{\rm min} \simeq 2.5 \left(\frac{M_{\rm t}}{M}\right)^{1/3} R, \quad (1)$$

★E-mail: derg@astro.cornell.edu (JF); dong@astro.cornell.edu (DL)

where M is the WD mass, $M_{\rm t} = M + M'$ is the total mass and R is the WD radius. This corresponds to orbital periods of

$$P \gtrsim P_{\rm min} = 68.4 \left(\frac{R}{10^4\,{\rm km}}\right)^{3/2} \left(\frac{M}{{\rm M}_\odot}\right)^{-1/2} {\rm s}. \quad (2)$$

Since WD g-mode periods are of the order of 1 min or longer, they can be excited by the binary companion prior to mass transfer. In particular, as the binary orbit decays due to gravitational radiation, the orbital frequency sweeps through a series of g-mode frequencies, transferring orbital energy to the modes. Although the overlap integral of the g-mode eigenfunctions with the tidal potential is generally quite small, a binary system that spends a long time at resonance can still excite g-modes to large amplitudes.

Previous studies of tidal interaction in WD binaries have focused on quasi-static tides (e.g. Iben, Tutukov & Fedorova 1998; Willems, Deloye & Kalogera 2010), which essentially correspond to non-resonant f-modes of the star. Such static tides become important only as the binary approaches the tidal limit (equation 1). Racine, Phinney & Arras (2007) recently studied non-dissipative tidal synchronization due to Rossby waves in accreting ultra-compact WD binaries. Rathore, Blandford & Broderick (2005) studied resonant mode excitations of WD modes in eccentric binaries. They focused on f-modes, for which the resonance occurs when harmonics of the orbital frequency matches the mode frequency. As mentioned above, for circular orbits, such resonance with the f-mode does not occur prior to mass transfer or tidal disruption. Their published analysis also did not include back reaction of the excited mode on the binary orbit.

The problem of resonant mode excitations in compact binaries has been studied before in the context of coalescing neutron star binaries: Reisenegger & Goldreich (1994), Lai (1994) and Shibata (1994) focused on the excitations of g-modes of non-rotating neutron stars; Ho & Lai (1999) and Lai & Wu (2006) studied the effects of NS rotation – including r-modes and other inertial modes; Flanagan & Racine (2007) examined gravitomagnetic excitation of r-modes. In the case of neutron star binaries, the orbital decay rate (for orbital frequencies larger than 5 Hz) is large and the mode amplitude is rather small, so the back reaction of the excited mode on the orbit can be safely neglected (see Section 5 of the present paper). By contrast, in the case of WD binaries, the orbital decay is much slower and the excited mode can reach a much larger amplitude. It thus becomes essential to take the back reaction into account.

In this paper, we consider WD binaries in circular orbits, consistent with the observed population of compact WD binaries (e.g. Kulkarni & van Kerkwijk 2010). Such circular orbits are a direct consequence of the circularization by gravitational radiation and/or the common envelope phase leading to their formation. A key assumption of this paper is that we assume the WD is not synchronized with the binary orbit. While it is true that the tidal circularization time-scale is much longer than the synchronization time, the observed circular orbit of the WD binaries does not imply synchronization. While there have been numerous studies of tidal dissipation in normal stars and giant planets (e.g. Zahn 1970, 1989; Goldreich & Nicholson 1977; Goodman & Oh 1997; Goodman & Dickson 1998; Ogilvie & Lin 2004, 2007; Wu 2005; Goodman & Lackner 2009), there has been no satisfactory study on tidal dissipation in WDs. Even for normal stars, the problem is not solved (especially for solar-type stars; see Goodman & Dickson 1998; see Zahn 2008 for review). In fact it is likely that the excitations of g-modes and other low-frequency modes play a role in the synchronization process. The orbital decay time-scale near g-mode resonances is relatively short (of the order of 10^4 yr for orbital periods of interest, i.e. minutes), so it is not clear that tidal synchronization can compete with the orbital decay rate. Given this uncertainty, we will consider non-rotating WDs (or slowly rotating WDs, so that the g-mode properties are not significantly modified by rotation) as a first step, and leaving the study of the rotational effects to a future paper.

This remainder of the paper is organized as follows. In Section 2 we present the equations governing the evolution of the orbit and the g-modes. Section 3 examines the properties of WD g-modes and their coupling with the tidal gravitational field of the companion. In Section 4, we numerically study the evolution of the g-modes through resonances and in Section 5 we present analytical estimates of the resonant g-mode excitation. We study the effect of mode damping on the tidal excitation in Section 6 and discuss the uncertainties and implications of our results in Section 7.

2 COMBINED EVOLUTION EQUATIONS FOR OSCILLATION MODES AND BINARY ORBIT

We consider a WD of mass M and radius R in orbit with a companion of mass M' (another WD, or NS or BH). The WD is non-spinning. The gravitational potential produced by M' can be written as

$$U(\boldsymbol{r}, t) = -\frac{GM'}{|\boldsymbol{r} - \boldsymbol{D}(t)|} = -GM' \sum_{lm} \frac{W_{lm} r^l}{D^{l+1}}\, {\rm e}^{-{\rm i}m\Phi(t)} Y_{lm}(\theta, \phi), \quad (3)$$

where $\boldsymbol{r} = (r, \theta, \phi)$ is the position vector (in spherical coordinates) of a fluid element in star M, $\boldsymbol{D}(t) = (D(t), \pi/2, \Phi(t))$ is the position vector of M' relative to M (D is the binary separation, Φ is the orbital phase or the true anomaly) and the coefficient W_{lm} is given by

$$W_{lm} = (-)^{(l+m)/2} \left[\frac{4\pi}{2l+1}(l+m)!(l-m)!\right]^{1/2} \times \left[2^l \left(\frac{l+m}{2}\right)! \left(\frac{l-m}{2}\right)!\right]^{-1}, \quad (4)$$

(Here the symbol $(-)^p$ is zero if p is not an integer.) The dominant $l = 2$ tidal potential has $W_{2\pm2} = (3\pi/10)^{1/2}$, $W_{20} = (\pi/5)^{1/2}$, $W_{2\pm1} = 0$, and so only the $m = \pm2$ modes can be resonantly excited.

The linear perturbation of the tidal potential on M is specified by the Lagrangian displacement $\boldsymbol{\xi}(\boldsymbol{r}, t)$, which satisfies the equation of motion

$$\frac{\partial^2 \boldsymbol{\xi}}{\partial t^2} + \mathcal{L} \cdot \boldsymbol{\xi} = -\nabla U, \quad (5)$$

where $\mathcal{L}$ is an operator that specifies the internal restoring forces of the star. The normal oscillation modes of the star satisfy $\mathcal{L} \cdot \boldsymbol{\xi}_\alpha = \omega_\alpha^2 \boldsymbol{\xi}_\alpha$, where $\alpha = \{n, l, m\}$ is the usual mode index and ω_α is the mode frequency. We write $\boldsymbol{\xi}(\boldsymbol{r}, t)$ as the sum of the normal modes:

$$\boldsymbol{\xi}(\boldsymbol{r}, t) = \sum_\alpha a_\alpha(t) \boldsymbol{\xi}_\alpha(\boldsymbol{r}). \quad (6)$$

The (complex) mode amplitude $a_\alpha(t)$ satisfies the equation

$$\ddot{a}_\alpha + \omega_\alpha^2 a_\alpha = \frac{GM' W_{lm} Q_\alpha}{D^{l+1}}\, {\rm e}^{-{\rm i}m\Phi(t)}, \quad (7)$$

where Q_α is the tidal coupling coefficient (also used by Press & Teukolsky 1977), defined by

$$\begin{aligned} Q_\alpha &= \left\langle \boldsymbol{\xi}_\alpha | \nabla \left(r^l Y_{lm} \right) \right\rangle \\ &= \int \mathrm{d}^3 x \ \rho \boldsymbol{\xi}_\alpha^* \cdot \nabla \left(r^l Y_{lm} \right) \\ &= \int \mathrm{d}^3 x \ \delta\rho_\alpha^* r^l Y_{lm}. \end{aligned} \tag{8}$$

Here $\delta\rho_\alpha = -\nabla \cdot (\rho \boldsymbol{\xi}_\alpha)$ is the Eulerian density perturbation. In deriving (7) we have used the normalization

$$\langle \boldsymbol{\xi}_\alpha | \boldsymbol{\xi}_\alpha \rangle = \int \mathrm{d}^3 x \rho \, \boldsymbol{\xi}_\alpha^* \cdot \boldsymbol{\xi}_\alpha = 1. \tag{9}$$

Resonant excitation of a mode α occurs when $\omega_\alpha = m\Omega$, where Ω is the orbital frequency.

In the *absence* of tidal interaction/resonance, the WD binary orbit decays due to gravitational radiation, with time-scale given by (Peters 1964)

$$\begin{aligned} t_D &= \frac{D}{|\dot{D}|} = \frac{5c^5}{64G^3} \frac{D^4}{M M' M_\mathrm{t}} \\ &= 3.2 \times 10^{10} \left(\frac{\mathrm{M}_\odot^2}{M M'} \right) \left(\frac{M_\mathrm{t}}{2\,\mathrm{M}_\odot} \right)^{1/3} \left(\frac{\Omega}{0.1\ \mathrm{s}^{-1}} \right)^{-8/3} \mathrm{s}, \end{aligned} \tag{10}$$

where $M_\mathrm{t} = M + M'$ is the total binary mass. When a strong tidal resonance occurs, the orbital decay rate can be modified, and we need to follow the evolution of the orbit and the mode amplitudes simultaneously. The gravitational interaction energy between M' and the modes in star M is

$$\begin{aligned} W &= \int \mathrm{d}^3 x \ U(\boldsymbol{r}, t) \sum_\alpha a_\alpha^*(t) \, \delta\rho_\alpha^*(\boldsymbol{r}) \\ &= -\sum_\alpha \frac{M' M R^2}{D^3} W_{lm} Q_\alpha \, \mathrm{e}^{-\mathrm{i}m\Phi} \, a_\alpha^*(t), \end{aligned} \tag{11}$$

where we have restricted to the $l = 2$ terms and set $G = 1$. The orbital evolution equations, including the effects of the modes, are then given by

$$\begin{aligned} \ddot{D} - D\dot{\Phi}^2 = &-\frac{M_\mathrm{t}}{D^2} - \sum_\alpha \frac{3M_\mathrm{t}}{D^4} W_{lm} Q_\alpha \ \mathrm{e}^{\mathrm{i}m\Phi} a_\alpha \\ &- \frac{M_\mathrm{t}}{D^2} \left(A_{5/2} + B_{5/2} \dot{D} \right), \end{aligned} \tag{12}$$

$$\begin{aligned} \ddot{\Phi} + \frac{2\dot{D}\dot{\Phi}}{D} = &\sum_\alpha \mathrm{i}m \frac{M_\mathrm{t}}{D^5} W_{lm} Q_\alpha \ \mathrm{e}^{\mathrm{i}m\Phi} a_\alpha \\ &- \frac{M_\mathrm{t}}{D^2} B_{5/2} \dot{\Phi}. \end{aligned} \tag{13}$$

The last terms on the right-hand side of equations (12) and (13) are the leading-order gravitational radiation reaction forces, with (see Lai & Wiseman 1996, and references therein).

$$A_{5/2} = -\frac{8\mu}{5D} \dot{D} \left(18v^2 + \frac{2M_\mathrm{t}}{3D} - 25\dot{D}^2 \right), \tag{14}$$

$$B_{5/2} = \frac{8\mu}{5D} \left(6v^2 - \frac{2M_\mathrm{t}}{D} - 15\dot{D}^2 \right), \tag{15}$$

where $\mu = MM'/M_\mathrm{t}$ and $v^2 = \dot{D}^2 + (D\dot{\Phi})^2$. In equations (12)–(15) we have set $G = c = 1$. We have dropped the other post-Newtonian terms since they have negligible effects on tidal excitations. The mode amplitude equation is given by equation (7), or,

$$\ddot{b}_\alpha - 2\mathrm{i}m\Omega\dot{b}_\alpha + \left(\omega_\alpha^2 - m^2\Omega^2 - \mathrm{i}m\dot{\Omega} \right) b_\alpha = \frac{M' W_{lm} Q_\alpha}{D^{l+1}}, \tag{16}$$

where

$$b_\alpha = a_\alpha \, \mathrm{e}^{\mathrm{i}m\Phi}. \tag{17}$$

3 WHITE DWARF G-MODES AND TIDAL COUPLING COEFFICIENTS

The non-radial adiabatic modes of a WD can be found by solving the standard stellar oscillation equations, as given in, e.g. Unno et al. (1989). The g-mode propagation zone in the star is determined by $\omega_\alpha^2 < N^2$ and $\omega_\alpha^2 < L_l^2$, where $L_l = \sqrt{l(l+1)} a_\mathrm{s}/r$ is the Lamb frequency (a_s is the sound speed), and N is the Brünt–Väisälä frequency, as given by

$$N^2 = g^2 \left[\frac{\mathrm{d}\rho}{\mathrm{d}P} - \left(\frac{\partial \rho}{\partial P} \right)_\mathrm{s} \right], \tag{18}$$

where g the gravitational acceleration, and the subscript 's' means that the adiabatic derivative is taken. Alternatively, N^2 can be obtained from (Brassard et al. 1991)

$$N^2 = \frac{\rho g^2 \chi_T}{P \chi_\rho} (\nabla_\mathrm{s} - \nabla + B), \tag{19}$$

where

$$\begin{aligned} \chi_T &= \left(\frac{\partial \ln P}{\partial ln T} \right)_{\rho, \{X_i\}}, \quad \chi_\rho = \left(\frac{\partial \ln P}{\partial \ln \rho} \right)_{T, \{X_i\}}, \\ \nabla &= \frac{\mathrm{d} \ln T}{\mathrm{d} \ln P}, \quad \nabla_\mathrm{s} = \left(\frac{\partial \ln T}{\partial \ln P} \right)_{\mathrm{s}, \{X_i\}}. \end{aligned} \tag{20}$$

The Ledoux term B accounts for the buoyancy arising from composition gradient:

$$B = -\frac{\chi_Y}{\chi_T} \frac{\mathrm{d} \ln Y}{\mathrm{d} \ln P}, \tag{21}$$

where

$$\chi_Y = \left(\frac{\partial \ln P}{\partial \ln Y} \right)_{\rho, T}, \tag{22}$$

and Y is the mass fraction of helium. This equation is valid for a compositional transition zone containing helium and one other element, as is the case for typical compositionally stratified DA WD models.

Fig. 1 shows the profiles of the Brünt Vaisälä and Lamb frequencies for one of the WD models adopted in this paper. These models were provided by G. Fontaine (see Brassard et al. 1991). Since the pressure in the WD core is almost completely determined by electron degeneracy pressure, $N^2 \propto \chi_T$ is very small except in the non-degenerate outer layers. As a result, g-modes are confined to the outer layers of the star below the convection zone. Lower-order modes have higher eigenfrequencies, so they are confined to regions where N^2 is especially large, i.e. just below the convection zone. Higher order modes have lower eigenfrequencies and can thus penetrate into deeper layers of the star where the value of N^2 is smaller. Cooler WDs have deeper convection zones that cause the modes to be confined to deeper layers where N^2 is smaller. Consequently, the eigenfrequencies and associated values of Q_α tend to be smaller in cooler WDs due to the decreased value of N^2 in the region of mode propagation.

The other feature of WDs that strongly effects their g-modes is their compositionally stratified layers. The sharp composition gradients that occur at the carbon–helium transition and the helium–hydrogen transition create large values of the Ledoux term B (equation 21), resulting in sharp peaks in N^2 as seen in Fig. 1. These

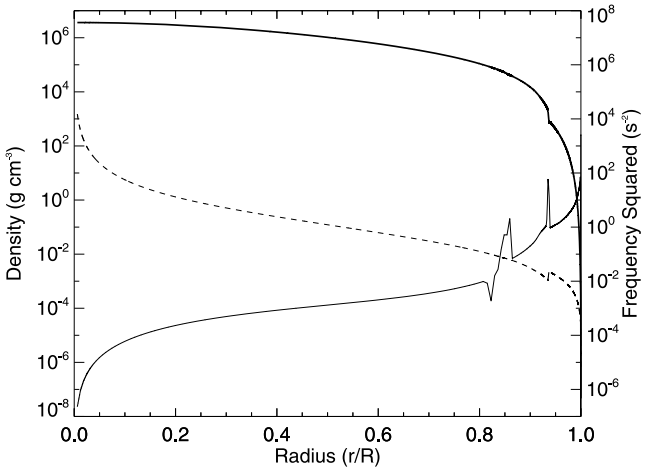

Figure 1. The square of the Brünt Väisälä (solid line) and Lamb (dotted line) frequencies and the density (thick solid line) as a function of normalized radius in a DA WD model, with $M = 0.6\,\mathrm{M}_\odot$, $R = 8.97 \times 10^3$ km, $T_{\rm eff} = 8720$ K. The spikes in the Brünt Väisälä frequency are caused by the composition changes from carbon to helium, and from helium to hydrogen, respectively.

peaks have a large effect on the WD g-modes, leading to phenomena such as mode-trapping (e.g. Brassard et al. 1992) and irregular period spectra. Thus, the eigenfrequencies and eigenfunctions of WD g-modes are very sensitive to WD models.

Tables 1–2 give the $l = 2$ f-mode and g-mode frequencies and their tidal coupling coefficients for two WD models. While the full oscillation equations need to be solved to accurately determine the f-modes, the Cowling approximation (in which the perturbation in the gravitational potential is neglected) gives accurate results for g-modes. Since high-order g-modes have rather small $|Q_\alpha|$, the mode eigenfunction must be solved accurately to obtain reliable Q_α. To ensure that this is achieved in our numerical integration, we use the orthogonality of the eigenfunctions to check the accuracy of the value of Q_α (see Reisenegger 1994 for a study on the general property of Q_α). Since the numerical determination of an eigenfunction is not perfect, it will contain traces of the other eigenfunctions, i.e.

$$(\boldsymbol{\xi}_\alpha)_{\rm num} = c_\alpha \boldsymbol{\xi}_\alpha + c_0 \boldsymbol{\xi}_0 + c_1 \boldsymbol{\xi}_1 + \cdots, \tag{23}$$

with $c_\alpha \simeq 1$ and $|c_\beta| \ll 1$ for $\beta \neq \alpha$. This means that the numerical tidal overlap integral is

$$\begin{aligned}(Q_\alpha)_{\rm num} &= \left\langle \nabla \left(r^l Y_{lm}\right) | (\boldsymbol{\xi}_\alpha)_{\rm num} \right\rangle \\ &= c_\alpha Q_\alpha + c_0 Q_0 + c_1 Q_1 + \ldots \end{aligned} \tag{24}$$

Since $|Q_0|$ (for the f-mode) is of order unity, while $|Q_\alpha| \ll 1$ for g-modes, to ensure $(Q_\alpha)_{\rm num}$ accurately represents the actual Q_α, we require

$$|c_0| \simeq |\langle \boldsymbol{\xi}_0 | \boldsymbol{\xi}_\alpha \rangle_{\rm num}| \ll |Q_\alpha|. \tag{25}$$

The results shown in Tables 1–2 reveal that $|c_0|$ is always more than an order of magnitude less than $\bar{Q}_\alpha$, so the above condition is satisfied for the modes computed in this paper.

We note from Tables 1–2 that while in general higher order g-modes tend to have smaller $|Q_\alpha|$, the dependence of $|Q_\alpha|$ on the mode index n is not exactly monotonic. This is the result of the mode trapping phenomenon associated with composition discontinuities in the WD. To see this, we note that a mode with amplitude $\boldsymbol{\xi}_\alpha$ has energy given by $E_\alpha = \omega_\alpha^2 \int \mathrm{d}^3 x \rho\, |\boldsymbol{\xi}_\alpha|^2$, thus we can define the mode energy weight function

$$\frac{\mathrm{d}E_\alpha}{\mathrm{d}\ln P} = \omega_\alpha^2 \rho\, r^2 \left[\xi_r^2 + l(l+1)\xi_\perp^2\right] H_{\rm p}, \tag{26}$$

where $H_{\rm p} = \mathrm{d}r/\mathrm{d}\ln P = P/(\rho g)$ is the pressure scale height, and we have used

$$\boldsymbol{\xi}_\alpha = [\xi_r(r)\,\mathbf{e}_r + r\xi_\perp(r)\nabla]\, Y_{lm} \tag{27}$$

($\mathbf{e}_r$ is the unit vector in the r-direction). Figs 2 and 3 display the weight functions for several g-modes of WD models. We can see that the weight functions for all the low-order modes are largest in the region below the convective zone near the spikes in N^2 produced by the composition gradients. For the modes shown in Fig. 2, the smooth fall-off of the weight function just below the convective zone indicates that these modes are confined by the falling value of the Lamb frequency in this region. The weight functions of higher order modes and the modes in WDs with deeper convective zones may drop sharply at the convective boundary, indicating that these modes are trapped by the convective zone rather than the decreasing Lamb frequency.

The weight functions also reveal the phenomenon known as mode trapping caused by the composition gradients. Mode trapping is especially evident for the $n = 2$ mode, as it is confined to the helium layer between the spikes in N^2. It is clear that the mode is reflected by the carbon–helium boundary at larger depths and by the helium–hydrogen boundary at shallower depths. See Brassard et al. (1992) for a more detailed description of the effects of mode trapping.

The weight function is essentially the energy of a mode as a function of radius, so it tells us where orbital energy is deposited when a mode is excited. Since the weight function is largest in the hydrogen and helium layers just below the convection zone, most of the mode energy exists in this region of the WD. Thus, if the

Table 1. The eigenfrequency $\bar{\omega}_\alpha$, tidal overlap parameter $\bar{Q}_\alpha$, and numerical f-mode overlap c_0 for the first six $l = 2$ g-modes of a white dwarf model. The white dwarf model has $T_{\rm eff} = 8720K$, $M = 0.6\,\mathrm{M}_\odot$, and $R = 8.97 \times 10^3$ km. Note that $\bar{\omega}_\alpha$ and $\bar{Q}_\alpha$ are in dimensionless units such that $G = M = R = 1$, and $(GM/R^3)^{1/2}/(2\pi) = 0.053$ Hz.

n	$\bar{\omega}_\alpha$	$\lvert\bar{Q}_\alpha\rvert$	c_0
0	2.08	0.428	1
1	0.298	1.27e-3	−1.80e-6
2	0.186	2.60e-3	3.91e-6
3	0.125	3.25e-5	3.62e-8
4	0.0900	8.91e-5	6.45e-7
5	0.0821	4.24e-4	1.32e-6
6	0.0715	6.91e-5	−2.54e-6

Table 2. Same as table 1, for a WD model of identical mass and composition but with $T_{\rm eff} = 5080$ K.

n	$\bar{\omega}_\alpha$	$\lvert\bar{Q}_\alpha\rvert$	c_0
0	2.01	0.439	1
1	0.251	1.00e-3	−2.03e-6
2	0.156	2.40e-3	−3.76e-6
3	0.107	1.79e-5	−1.25e-7
4	0.0723	1.53e-5	4.95e-7
5	0.0537	8.42e-5	1.52e-6
6	0.0513	1.26e-4	1.42e-6

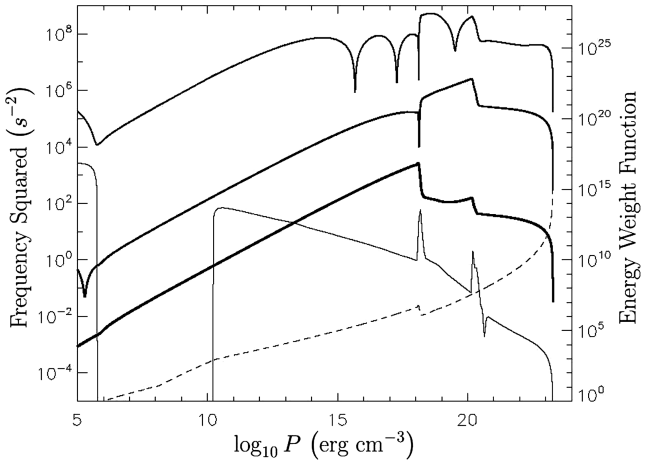

Figure 2. The mode energy weight functions for the $n = 1$ (thickest line), $n = 2$ (thick line) and $n = 5$ (top line) modes (all for $l = 2$) for a WD with $T_{\rm eff} = 8720$ K, $M = 0.6\,{\rm M}_{\odot}$, $R = 8.97 \times 10^3$ km, displayed as a function of log$P$ so that the structure of the outer layers of the WD is more evident. The y-axis for a given mode is intended only to show the relative value of the weight function. The squares of the Brünt Väisälä (thin solid line) and Lamb (dotted line) frequencies are displayed to demonstrate how their values constrain the region of mode propagation.

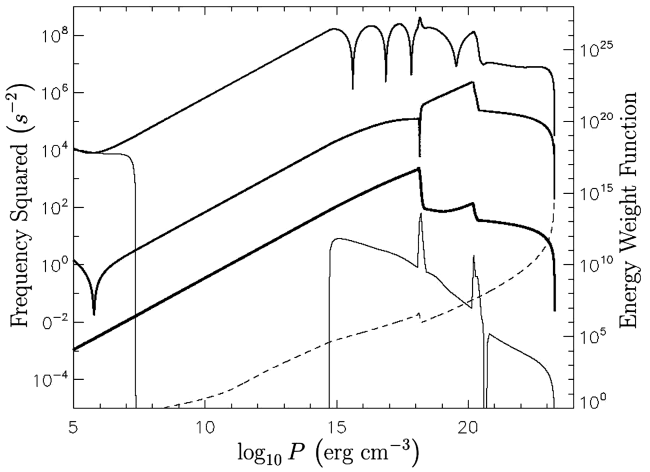

Figure 3. Same as Fig. 2, except for a WD model with $T_{\rm eff} = 5080$ K. Note that the convection zone extends deeper in this model, pushing the modes to larger depths.

mode is damped, most of the mode energy will be damped out in this region.

4 NUMERICAL RESULTS FOR MODE-ORBIT EVOLUTION THROUGH RESONANCE

Having obtained the mode frequency and the tidal coupling coefficient, we can determine the combined evolution of the resonant mode and the binary orbit using equations (7), (12) and (13). These are integrated from well before resonance until well after the resonance is complete. The initial mode amplitude b_α and its derivative $\dot{b}_\alpha$ (prior to a resonance) are obtained by dropping the $\ddot{b}_\alpha$, $\dot{b}_\alpha$ and $\dot{\Omega}$ terms in equation (16), giving

$$b_\alpha \simeq \frac{M' W_{lm} Q_\alpha}{D^{l+1}\left(\omega_\alpha^2 - m^2\Omega^2\right)}, \tag{28}$$

$$\dot{b}_\alpha \simeq \left[-(l+1)\frac{\dot{D}}{D} + \frac{2m^2\Omega\dot{\Omega}}{\omega_\alpha^2 - m^2\Omega^2}\right] b_\alpha, \tag{29}$$

with $\dot{\Omega} \simeq -(3\dot{D}/2D)\Omega$. These expressions are valid for for $(\omega_\alpha/m\Omega)^2 - 1 \gg \dot{\Omega}/(m\Omega^2) \simeq 3/(2m\Omega t_D)$ (see Section 5).

The evolution equations (7), (12) and (13) form a very stiff set of differential equations. The reason for this is that the problem involves two vastly different time scales: the orbital decay time-scale which is on the order of thousands of years, and the orbital time-scale (or the resonant mode oscillation period) which is on the order of minutes. Consequently, a typical Runge–Kutta scheme would require the integration of millions of orbits, demanding a high degree of accuracy for each orbit. To avoid this problem, we employ the Rossenberg stiff equation technique (Press et al. 2007). The integrator requires a Jacobian matrix of second derivatives, meaning that we need to supply the 8×8 matrix of second derivatives corresponding to our eight first-order differential equations. The evolution equations are sufficiently simple that this matrix can be found analytically.

Fig. 4 depicts an example of the mode amplitude and orbit evolution near the resonance for the $n = 3$ g-mode. Before the resonance, the mode must oscillate with the same frequency as the binary companion, so the amplitude $|b_\alpha|$ is smooth. After the resonance, the mode oscillates at its eigenfrequency (which is now different from the forcing frequency). The amplitude of the mode continues to fluctuate after resonance because it is still being forced by the binary companion, although the amplitude of these fluctuations diminishes over time as the orbit moves further from resonance.

Fig. 5 displays the average post-resonance amplitudes for the first five modes given in Table I. Note that no mode exceeds a maximum amplitude of $|b_\alpha| = 0.1$, and we expect that our linear approximation is a reasonable first approach to the problem before non-linear effects can be included. In general, lower order modes reach larger amplitudes (due to their larger coupling coefficients), but higher order modes with an abnormally high value of Q_α (trapped modes) may reach large amplitudes as well.

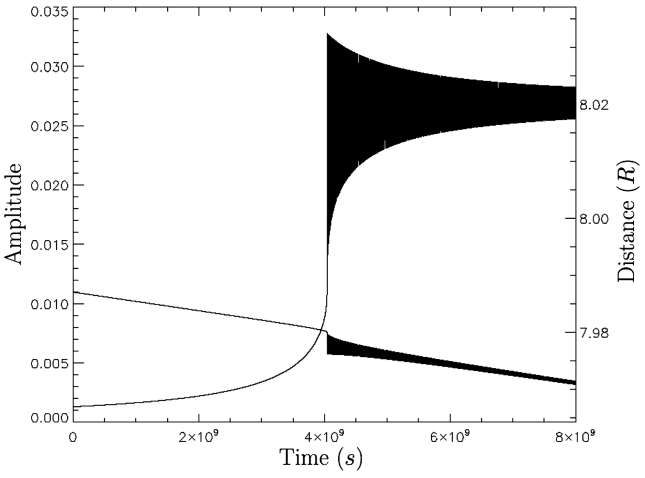

Figure 4. Mode amplitude $|b_\alpha|$ and orbital distance D as a function of time during resonance. The amplitude and distance oscillate after resonance, causing the curves to appear as filled shapes due to the short period of the oscillations with respect to the total integration time. These oscillations occur due to the continued interaction between the excited mode and the orbit. Note the sharp drop in orbital distance at resonance, which is caused by the transfer of orbital energy into the mode. The mode parameters are given in Table I ($n = 3$). The companion mass is $M' = M = 0.6\,{\rm M}_{\odot}$.

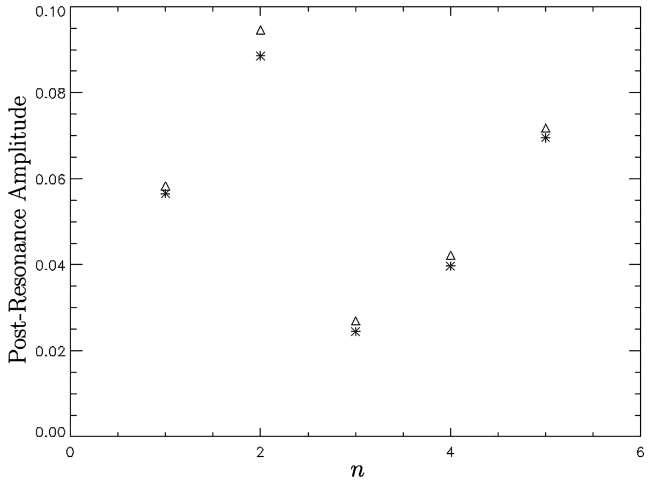

Figure 5. The average post-resonance amplitudes for the first five modes given in Table I. The open triangles mark the results obtained from numerical integration, and the asterisks indicate the results predicted by the analytical estimate described in Section 5. The analytical estimates are usually accurate within a factor of 10 per cent. The $n = 2$ and 5 modes are trapped modes.

5 ANALYTIC ESTIMATE OF THE RESONANT MODE AMPLITUDE

Here we provide an analytic estimate of the mode amplitude attained during a resonance as well as the temporal duration of the resonance (i.e. the characteristic time during which the resonant mode receives most of its energy from the orbit).

For a WD oscillation mode with frequency ω_α, the resonant orbital radius is

$$D_\alpha = \left(\frac{m^2 M_{\rm t}}{\omega_\alpha^2}\right)^{1/3}. \tag{30}$$

Prior to the resonance, as the orbital radius D decreases, the mode amplitude grows gradually according to equation (28). At the same time, the orbit also loses its energy to GWs at the rate

$$\dot{E}_{\rm GW} = -\frac{32(MM')^2 M_{\rm t}}{5c^5 D^5} = -\frac{MM'/2D}{t_D}, \tag{31}$$

where t_D is given by equation (10). We can define the beginning of resonance as the point where the orbital energy is transferred to the mode faster than it is radiated away by GWs. That is, the resonance begins at the radius $D = D_{\alpha+}(>D_\alpha)$, as determined by

$$\dot{E}_\alpha = |\dot{E}_{\rm GW}|, \tag{32}$$

where E_α is the energy contained in the mode. Near the resonance, the mode oscillates at the frequency close to ω_α, so we can write the mode energy as $E_\alpha \simeq 2\omega_\alpha^2 b_\alpha^2$ (including both the $m = 2$ and $m = -2$ terms), assuming $\omega_\alpha \gg |\dot{b}_\alpha/b_\alpha|$. Thus we have $\dot{E}_\alpha \simeq 4\omega_\alpha^2 b_\alpha \dot{b}_\alpha$. Using equations (28) and (29) for b_α and $\dot{b}_\alpha$, we find

$$\omega_\alpha^2 - (m\Omega)^2 = \left[\frac{24\omega_\alpha^4 M'(W_{lm} Q_\alpha)^2}{MD^5}\right]^{1/3} \quad \text{at} \quad D = D_{\alpha+} \tag{33}$$

or

$$D_{\alpha+} = D_\alpha \left[1 + 0.436\left(\frac{M'}{M}\right)^{1/3}\left(\frac{M_{\rm t}}{M}\right)^{-5/9} \bar{\omega}_\alpha^{4/9} \bar{Q}_\alpha^{2/3}\right], \tag{34}$$

where we have used $l = m = 2$ and $\bar{\omega}_\alpha$, $\bar{Q}_\alpha$ are in dimensionless units where $G = M = R = 1$. The mode energy at $D = D_{\alpha+}$ is

$$E_\alpha(D_{\alpha+}) = 0.0701\left(\frac{M'}{M}\right)^{4/3}\left(\frac{M_{\rm t}}{M}\right)^{-8/9} \times \bar{\omega}_\alpha^{10/9}(W_{lm}\bar{Q}_\alpha)^{2/3}\frac{M^2}{R}. \tag{35}$$

Since for $D < D_{\alpha+}$, the orbital energy will be deposited into the mode much faster than it is being radiated away, we approximate that all the orbital energy between $D_{\alpha+}$ and D_α is transferred to the mode. Thus the mode energy increases by the amount

$$\Delta E_\alpha = 2 \times \left(\frac{MM'}{2D_\alpha} - \frac{MM'}{2D_{\alpha+}}\right), \tag{36}$$

where we have multiplied by a factor of two to account for the fact that energy is also deposited at a nearly equal rate before resonance as it is after resonance. Using equation (34), we find

$$\Delta E_\alpha = 0.2804\left(\frac{M'}{M}\right)^{4/3}\left(\frac{M_{\rm t}}{M}\right)^{-8/9} \times \bar{\omega}_\alpha^{10/9}(W_{lm}\bar{Q}_\alpha)^{2/3}\frac{M^2}{R}. \tag{37}$$

This is exactly four times of equation (35). Thus the maximum mode energy after resonance is $E_{\alpha,\max} = E_\alpha(D_{\alpha+}) + \Delta E_\alpha$, or

$$E_{\alpha,\max} \simeq 5.75\times 10^{-4}\left(\frac{M'}{M}\right)^{4/3}\left(\frac{M_{\rm t}}{M}\right)^{-8/9} \times \left(\frac{\bar{\omega}_\alpha}{0.2}\right)^{10/9}\left(\frac{\bar{Q}_\alpha}{10^{-3}}\right)^{2/3}\frac{M^2}{R}. \tag{38}$$

The corresponding maximum mode amplitude is

$$b_{\alpha,\max} \simeq 8.48\times 10^{-2}\left(\frac{M'}{M}\right)^{2/3}\left(\frac{M_{\rm t}}{M}\right)^{-4/9} \times \left(\frac{\bar{\omega}_\alpha}{0.2}\right)^{-4/9}\left(\frac{\bar{Q}_\alpha}{10^{-3}}\right)^{1/3}. \tag{39}$$

Figs 5 and 6 compare our numerical results with the analytical expressions (38)–(39). We find good agreement for all the WD resonant modes considered. Fig. 5 verifies the dependence of $b_{\alpha,\max}$

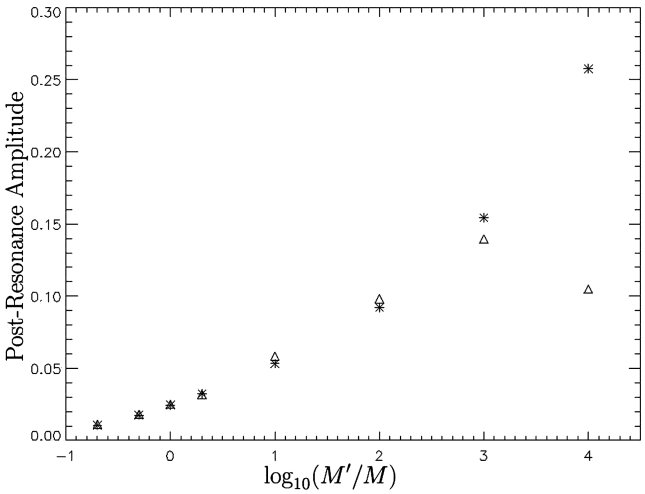

Figure 6. The average post-resonance amplitude $|b_\alpha|$ for the $n = 4$ mode given in Table I as a function of the mass of the binary companion. The post-resonance amplitude increases with the mass of the binary companion as predicted by the analytical estimate except for very high companion masses.

on the mode frequency and the value of $\bar{Q}_\alpha$, while Fig. 6 verifies the dependence of $b_{\alpha,\max}$ on the mass of the binary companion (except for the highest mass cases discussed below). Therefore equations (38) and (39) provide fairly accurate estimates of the mode amplitude and energy without performing numerical integrations.

For the very high companion masses ($M' \gtrsim 10^3 M$) shown in Fig. 6, our analytical formula significantly overestimates the post-resonance amplitude. The reason for this is that the gravitational decay time-scale is shorter if the companion is more massive. If the companion is massive enough, the orbit will decay through resonance due to gravitational radiation before the orbital energy of equation (37) can be deposited in the mode (see below). Consequently, the amplitude to which a mode is excited decreases if the mass of the companion becomes very high. Therefore our analytical formula overestimates the post-resonance amplitude for extremely massive companions. For any reasonable WD or NS masses, our analytical estimate is accurate, but for a super-massive black hole the estimate may become inaccurate.

It is interesting that the above analytical results for the resonant mode energy is independent of the GW damping time-scale t_D, in contrast to the NS/NS or NS/BH binary cases. In fact, for the above derivation to be valid, the following four conditions must be satisfied at $D_{\alpha+}$:

$$\text{(i)}\ \ \omega_\alpha \gg |\dot{b}_\alpha / b_\alpha|, \tag{40}$$

$$\text{(ii)}\ \ \omega_\alpha^2 - (m\Omega)^2 \gg m\dot{\Omega}, \tag{41}$$

$$\text{(iii)}\ \ \omega_\alpha^2 - (m\Omega)^2 \gg 2m\Omega|\dot{b}_\alpha / b_\alpha|, \tag{42}$$

$$\text{(iv)}\ \ \omega_\alpha^2 - (m\Omega)^2 \gg |\ddot{b}_\alpha / b_\alpha|. \tag{43}$$

Conditions (i) and (ii) both lead to

$$\omega_\alpha t_D \gg 3\left[\frac{\omega_\alpha^2}{\omega_\alpha^2 - (m\Omega)^2}\right]; \tag{44}$$

condition (iii) gives

$$\omega_\alpha t_D \gg 6\left[\frac{\omega_\alpha^2}{\omega_\alpha^2 - (m\Omega)^2}\right]^2; \tag{45}$$

and condition (iv) yields

$$\omega_\alpha t_D \gg \sqrt{18}\left[\frac{\omega_\alpha^2}{\omega_\alpha^2 - (m\Omega)^2}\right]^{3/2}. \tag{46}$$

In equations (44)–(46), the right-hand sides should be evaluated at $D_{\alpha+}$. Clearly, condition (iii) is most constraining. With

$$\frac{\omega_\alpha^2 - (m\Omega)^2}{\omega_\alpha^2} = 3\left(\frac{D_{\alpha+} - D_\alpha}{D_\alpha}\right) = 0.0064\left(\frac{M'}{M}\right)^{1/3}\left(\frac{M_{\rm t}}{M}\right)^{-5/9}\left(\frac{\bar{\omega}_\alpha}{0.2}\right)^{4/9}\left(\frac{\bar{Q}_\alpha}{10^{-3}}\right)^{2/3}, \tag{47}$$

we see that condition (iii) is satisfied if

$$t_D \gg 7.3\times 10^5\left(\frac{R^3}{GM}\right)^{1/2}\left(\frac{M'}{M}\right)^{-2/3}\left(\frac{M_{\rm t}}{M}\right)^{10/9} \times \left(\frac{\bar{\omega}_\alpha}{0.2}\right)^{-17/9}\left(\frac{\bar{Q}_\alpha}{10^{-3}}\right)^{-4/3}. \tag{48}$$

Since t_D is on the order of a thousand years or more for orbital frequencies comparable to WD g-modes, condition (iii) is always satisfied for WD/WD or WD/NS binaries. On the other hand, the conditions (i)–(iv) are not all satisfied for NS/NS or NS/BH binaries.

For very massive companions, the inequality of equation (48) may not hold. Using equation (10) for t_D, equation (48) implies (for $M_{\rm t}/M \simeq M'/M$)

$$\frac{M'}{M} \ll 5.5\times 10^4\left(\frac{\bar{\omega}_\alpha}{0.2}\right)^{-7/10}\left(\frac{\bar{Q}_\alpha}{10^{-3}}\right)^{6/5} \times \left(\frac{M}{\rm M_\odot}\right)^{-9/4}\left(\frac{R}{10^4\,\rm km}\right)^{9/4}. \tag{49}$$

The above inequality implies our estimates are valid for any feasible companion except a super-massive black hole.[1] We can also use this inequality to examine the inaccuracy of our estimate in the highest mass cases of Fig. 6. Fig. 6 was generated using the $n = 3$ mode parameters listed in Table 1 for a WD of $M = 0.6\,\rm M_\odot$ and $R = 8.97\times 10^3$ km. Plugging in these parameters, equation (49) requires

$$\frac{M'}{M} \ll 1.7\times 10^3 \tag{50}$$

for our analytical estimates in Fig. 6 to be accurate. This explains why the analytical estimates of Fig. 6 are accurate when $M' \lesssim 1000M$ but diverge from the numerical results when $M' \gtrsim 1000M$.

Given the maximum mode amplitude reached during a resonance, we can now estimate the temporal duration of the resonance. Letting $a_\alpha = c_\alpha e^{-i\omega_\alpha t}$, the mode amplitude evolution equation (7) becomes

$$\ddot{c}_\alpha - 2i\omega_\alpha \dot{c}_\alpha = \frac{M' W_{lm} Q_\alpha}{D^3} e^{i\omega_\alpha t - im\Phi}. \tag{51}$$

Assuming that during the resonance, $\omega_\alpha - m\Omega \simeq 0$, the right-hand side of equation (51) can be taken as a constant, we then have

$$\dot{c}_\alpha \simeq \frac{iM' W_{lm} Q_\alpha}{2\omega_\alpha D^3}, \tag{52}$$

i.e. the mode amplitude grows linearly in time. Thus, the duration of the resonance is of order

$$t_{\rm res} = \left|\frac{b_{\alpha,\max}}{\dot{c}_\alpha}\right| \simeq 3.42\left(\frac{M'}{M}\right)^{-1/3}\left(\frac{M_{\rm t}}{M}\right)^{5/9}\bar{\omega}_\alpha^{-13/9}\bar{Q}_\alpha^{-2/3}\left(\frac{R^3}{M}\right)^{1/2} = 3.50\times 10^3\left(\frac{M'}{M}\right)^{-1/3}\left(\frac{M_{\rm t}}{M}\right)^{5/9} \times \left(\frac{\bar{\omega}_\alpha}{0.2}\right)^{-13/9}\left(\frac{\bar{Q}_\alpha}{10^{-3}}\right)^{-2/3}\left(\frac{R^3}{M}\right)^{1/2}. \tag{53}$$

Since the dynamical time $(R^3/GM)^{1/2}$ for typical WDs is on the order of 1s, the resonance duration is typically an hour or longer. Note that the above estimate is formally valid only when $[\omega - m\Omega(D_{\alpha+})]t_{\rm res} \ll 1$, so that we can set $\omega_\alpha - m\Omega \approx 0$ for the duration of the resonance. Using equations (47) and (53), we find $[\omega_\alpha - m\Omega(D_{\alpha+})]t_{\rm res} \approx 1$ for typical parameters. Thus we should consider equation (53) as an order-of-magnitude estimate only. Also, we can check that the GW energy loss during the resonance, $\Delta E_{\rm gw} \simeq (MM'/2D_\alpha)(t_{\rm res}/t_D)$, is much less than $E_{\alpha,\max}$, justifying our derivation of $E_{\alpha,\max}$ given by equation (38). Indeed, the above condition simplifies to equation 49, since in both cases it is the energy carried away by GWs that is limiting the mode growth.

We can use the same method to solve for the size of the fluctuations in mode amplitude after resonance. Due to the symmetry

[1] Obviously, our estimate would not apply for a WD in a highly eccentric orbit around an intermediate mass black hole, which may form in dense clusters as described by Ivanov & Papaloizou (2007).

of the harmonic oscillator, the fluctuation in mode amplitude about the mean value after the resonance is identical to the zeroth-order estimate of the mode amplitude before resonance (see equation 28), i.e.

$$\Delta a \approx \frac{M' W_{lm} Q_\alpha}{D^{l+1}\left(m^2\Omega^2 - \omega_\alpha^2\right)}. \tag{54}$$

These fluctuations occur with frequency $m\Omega - \omega_\alpha$, since this is the difference in frequency between the eigenfrequency at which the WD is oscillating and the orbital forcing frequency. So, as the orbital frequency continues to increase after the resonance, the amplitude of the fluctuations becomes smaller while the frequency of the amplitude oscillations becomes higher.

6 EFFECT OF MODE DAMPING

The results in the previous two sections neglect mode energy damping in the WD. Since the duration of the resonance is much longer than the mode period (see equation 53), internal mode damping could affect the energy transfer during resonance if the damping rate is sufficiently large. To address this issue, we incorporate a phenomenological damping rate $-\gamma_\alpha \omega_\alpha \dot{a}_\alpha$ to the mode equation (7) to study how mode damping affects energy transfer during a resonance. Fig. 7 shows the excitation of a mode through resonance for different values of γ_α. We see that, as expected, when the internal damping time is larger than the resonance duration (equation 53), the maximum mode energy achieved in a resonance is unaffected.

G-modes in white dwarfs are damped primarily by radiative diffusion. For sufficiently large mode amplitudes, non-linear damping is also important (e.g. Kumar & Goodman 1996; see Section 7 for more discussion on this issue). Wu (1998) presents estimates for the non-adiabatic radiative damping rates of WD g-modes in terms of $\omega_i = \gamma\omega_r$. Extrapolating Wu's values to $l = 2$ modes for a white dwarf of temperature $T = 8720\,\mathrm{K}$, we find $\gamma \sim 10^{-11}$ for modes near $n = 1$ and $\gamma \sim 10^{-4}$ for high-order modes with $n \gtrsim 20$. So, while the maximum amplitude of low-order modes is completely unaffected by non-adiabatic effects, high-order modes will damp on time scales similar to the excitation time-scale. Therefore these high-order modes will attain amplitudes somewhat smaller than estimated in the previous section. This continual process of high-order mode damping may extract energy out of the orbit more efficiently than discrete resonance events, causing a steady decay of the binary's orbit.

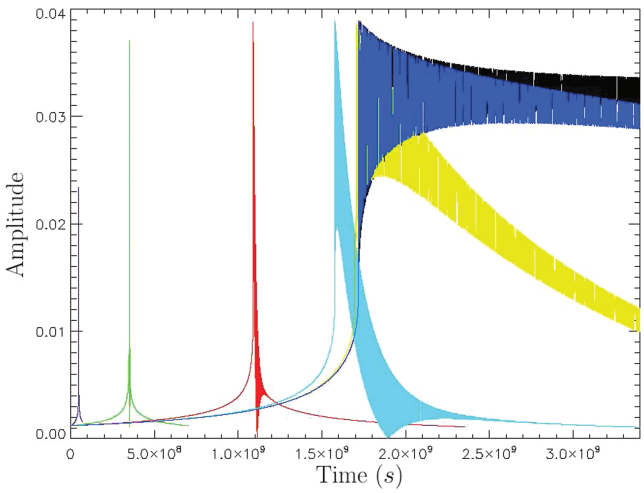

Figure 7. The amplitude of a mode as a function of time near its resonance for different values of the damping coefficient γ_α. The curves have $\gamma_\alpha = 0$ (black), $\gamma_\alpha = 10^{-9}$ (dark blue), $\gamma_\alpha = 10^{-8}$ (yellow-green), $\gamma_\alpha = 10^{-7}$ (light blue), $\gamma_\alpha = 10^{-6}$ (red), $\gamma_\alpha = 10^{-5}$ (green), and $\gamma_\alpha = 10^{-4}$ (purple). For this mode, we have set $\omega_\alpha = 0.1\ \mathrm{s}^{-1}$ and $Q_\alpha = 1 \times 10^{-4}$ so that $t_{\rm res} \approx 10^5$ s. Note that the damping term does not greatly affect the maximum mode amplitude except when $\gamma_\alpha \gtrsim 10^{-4}$, or when $\gamma_\alpha \omega_\alpha t_{\rm res} \gtrsim 1$. Also note that modes with larger values of γ_α evolve on a much shorter time-scale because their orbits decay quickly due to the conversion of orbital energy into heat via mode damping.

7 DISCUSSION

We have shown that during the orbital decay of compact white dwarf binaries (WD/WD, WD/NS or WD/BH), a series of g-modes can be tidally excited to large amplitudes (up to 0.1 in dimensionless units) as the orbital frequency sweeps through the resonant mode frequencies. Such mode excitations can significantly affect the orbital decay rate near resonance. Indeed, to properly calculate the resonant mode amplitude, it is necessary to take into account of the back-reaction of the excited modes on the orbit. One consequence of the resonant mode excitations is that the low-frequency ($\lesssim 10^{-2}$ Hz) gravitational waveforms emitted by the binary, detectable by LISA, will deviate significantly from the point-mass binary prediction. This is in contrast to the case of neutron star binaries (NS/NS or NS/BH) studied previously (Lai 1994; Reisenegger & Goldreich 1994; Shibata 1994; Ho & Lai 1999; Flanagan & Racine 2007; Lai & Wu 2006), where the resonant mode amplitude is normally too small to affect the binary orbital decay rate and the gravitational waveforms to be detected by ground-based GW detectors such as LIGO and VIRGO.

In the case of WD binaries studied in this paper, the number of of orbits skipped as a result of a resonant mode excitation is

$$\Delta N_{\rm orb} = \frac{t_D}{P_{\rm orb}} \frac{E_{\alpha,\max}}{E_{\rm orb}}, \tag{55}$$

where t_D is the GW decay time-scale given in equation (10), $P_{\rm orb}$ is the orbital period, and $E_{\rm orb}$ is the orbital energy at resonance. Using equation (38) for $E_{\alpha,\max}$, we find

$$\Delta N_{\rm orb} = 3.4 \times 10^6 \left(\frac{\mathrm{M}_\odot^{17}}{M^9 M'^6 M_{\rm t}^2}\right)^{1/9} \times \left(\frac{R}{10^4\,\mathrm{km}}\right)^{2/3} \left(\frac{\bar{Q}_\alpha}{10^{-3}}\right)^{2/3} \left(\frac{\Omega}{0.1\,\mathrm{s}^{-1}}\right)^{-11/9}. \tag{56}$$

The number of skipped orbital cycles should be compared to the number of orbits in a decay time, expressed by

$$\frac{\mathrm{d}N_{\rm orb}}{\mathrm{d}\ln\Omega} = \frac{2}{3}\Omega t_D = 2.1 \times 10^9 \left(\frac{\mathrm{M}_\odot^2}{MM'}\right)\left(\frac{M_{\rm t}}{2\,\mathrm{M}_\odot}\right)^{1/3}\left(\frac{\Omega}{0.1\,\mathrm{s}^{-1}}\right)^{-5/3}. \tag{57}$$

The huge number of skipped orbital cycles implies that such a resonant interaction would be important, but because the number of skipped orbital cycles is much smaller than the number of orbital cycles in a decay time, resonances will not dominate the decay process.

A second possible consequence of resonant mode excitations is that the large mode energy may lead to significant heating of the white dwarf prior to the binary merger. Indeed, equation (38) shows that for typical binary parameters, the mode energy can be a significant fraction ($\sim 10^{-4}$–10^{-3}) of the gravitational binding

energy of the star, and comparable to the thermal energy. Indeed, the thermal energy of the WD is of order $E_{\rm th} \approx \frac{MkT_{\rm c}}{Am_p}$, where $T_{\rm c}$ is the core temperature of the WD and A is the mean atomic weight. The ratio of post-resonance mode energy to thermal energy is then

$$\frac{E_{\alpha,\max}}{E_{\rm th}} \approx 1.7 \left(\frac{M'}{M}\right)^{4/3} \left(\frac{M_{\rm t}}{M}\right)^{-8/9} \left(\frac{\bar{\omega}_\alpha}{0.2}\right)^{10/9} \times \left(\frac{\bar{Q}_\alpha}{10^{-3}}\right)^{2/3} \left(\frac{10^7 K}{T_{\rm c}}\right) \left(\frac{M}{\rm M_\odot}\right) \left(\frac{10^4\,{\rm km}}{R}\right). \quad (58)$$

This implies that the white dwarf may become bright thousands of years before binary merger.

A third consequence that may result from a resonance is significant spin-up of the WD. If we assume that all the angular momentum transferred to the WD during a resonance eventually manifests as rigid body rotation of the WD, the change in spin frequency of the WD is

$$\Delta\Omega_{\rm s} = \frac{E_{\alpha,\max}}{I\Omega}, \quad (59)$$

where $\Omega_{\rm s}$ is the spin frequency of the WD and I is its moment of inertia. Plugging in our expression for $E_{\alpha,\max}$, we find

$$\Delta\Omega_{\rm s} = 0.29 \left(\frac{0.2}{\kappa}\right) \left(\frac{M'}{M}\right)^{4/3} \left(\frac{M_{\rm t}}{M}\right)^{-8/9} \times \left(\frac{\bar{\omega}_\alpha}{0.2}\right)^{-8/9} \left(\frac{\bar{Q}_\alpha}{10^{-3}}\right)^{2/3} \Omega, \quad (60)$$

where $\kappa = I/(MR^2) \approx 0.2$. We can thus see that a given resonance may deposit enough angular momentum to completely spin-up the WD (or significantly alter its spin) by the time the mode damps out. This implies that mode resonances are potentially very important in the spin synchronization process.

However, before these implications can be taken seriously, one should be aware of the limitations of the present study. One issue is the assumption that the white dwarf is non-rotating (and not synchronized), already commented on in Section 1. More importantly, we have assumed that the white dwarf oscillations can be calculated in the linear regime. While the mass-averaged dimensionless amplitude $|a_\alpha| = |b_\alpha|$ of the excited g-mode is less than 0.1 (see Fig. 5 and equation 39), the physical fluid displacement in the stellar envelope is much larger since g-modes of white dwarfs are mainly concentrated in the outer, non-degenerate layers. Fig. 8 gives some examples: it shows the horizontal and radial displacements of three modes at their post-resonance amplitudes. These are obtained from $\boldsymbol{\xi} = a_\alpha \boldsymbol{\xi}_\alpha$, with $\boldsymbol{\xi}_\alpha$ the normalized eigenfunction (see Section 3) and a_α computed from equation (39) with $M' = M$. In general, the linear approximation is valid only if $|\boldsymbol{\xi}| \ll |k_r|^{-1}$, where k_r is the WKB wavenumber, given by

$$k_r^2 \simeq \frac{l(l+1)(N^2-\omega^2)}{\omega^2 r^2}. \quad (61)$$

Clearly, the three modes depicted in Fig. 8 strongly violate the linear approximation beyond the radius $r \approx 0.85R$, near the jump in N^2 associated with the carbon–helium boundary.

Therefore, the results presented in this paper should be treated with caution as non-linear effects will likely limit mode growth. Rather than increasing to the large displacements shown in Fig. 8, the white dwarf oscillations will undergo non-linear processes such as mode coupling that will transfer energy to high-order modes. These high-order modes have much shorter wavelengths and thus damp on very short time scales. As non-linearity is most important in the outer layers of the white dwarf, we expect that the excited oscillation will dissipate its energy preferentially in this outer layer and will not reflect back into the stellar interior. We plan to address these issues in our next paper (Fuller & Lai, in preparation).

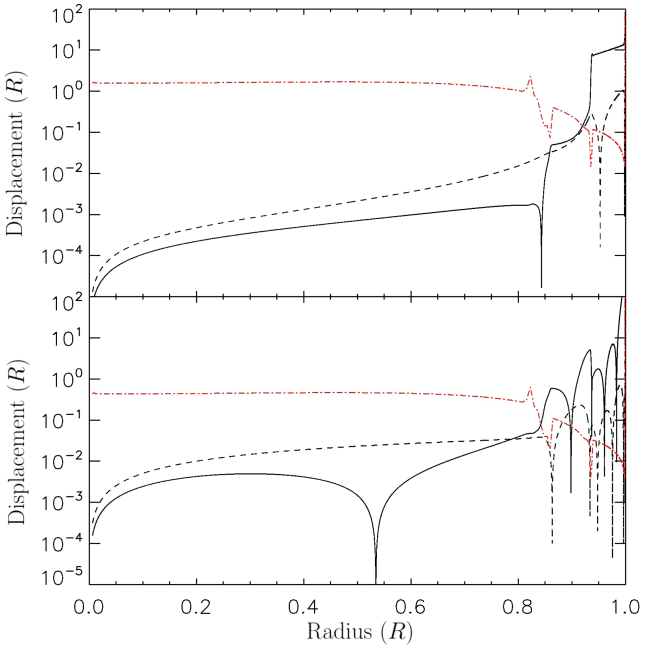

Figure 8. The horizontal (solid line) and radial (dashed line) displacements of the $n = 1$ (top panel) and $n = 5$ (bottom panel) modes as a function of radius. The physical displacements are calculated using the analytical estimates for the post-resonance amplitudes given in equation 39 using $M = M'$, giving $|a_1| = 0.0566$ and $|a_5| = 0.0695$. Also shown is inverse of the WKB wavenumber $1/k_r$ (dotted line).

ACKNOWLEDGMENTS

We thank Gilles Fontaine (University of Montreal) for providing the white dwarf models used in this paper and for valuable advice on these models. DL thanks Lars Bildsten, Gordon Ogilvie and Yanqin Wu for useful discussions, and acknowledges the hospitality of the Kavli Institute for Theoretical Physics at UCSB (funded by the NSF through Grant PHY05-51164) where part of the work was carried out. This work has been supported in part by NASA Grant NNX07AG81G and NSF grants AST 0707628.

REFERENCES

Badenes C., Mullally F., Thompson S. E., Lupton R. H., 2009, ApJ, 707, 971
Brassard P., Fontaine G., Wesemael F., Kwaler S. D., Tassoul M., 1991, ApJ, 367, 601
Brassard P., Fontaine G., Wesemael F., Hansen C. J., 1992, ApJS, 80, 369
Brickhill A. J., 1983, MNRAS, 204, 537
Flanagan E., Racine E., 2007, Phys. Rev. D, 75, 044001
Goodman J., Lackner C., 2009, ApJ, 696, 2054
Goldreich P., Nicholson P., 1977, Icarus, 30, 301
Goldreich P., Wu Y., 1999, ApJ, 511, 904
Goodman J., Dickson E. S., 1998, ApJ, 507, 938
Goodman J., Oh S. P., 1997, ApJ, 486, 403
Ho W. C. G., Lai D., 1999, MNRAS, 308, 153
Iben I., Tutukov A., Fedorova A., 1998, ApJ, 503, 344
Ivanov P. B., Papaloizou J. C. B., 2007, A&A, 476, 121
Kilic M., Brown W. R., Allende Prieto C., Swift B., Kenyon S. J., Liebert J., Agueros M. A., 2009, ApJ, 695, L92

Kulkarni S. R., van Kerkwijk M. H., 2010, ApJ, 719, 1123
Kumar P., Goodman J., 1996, ApJ, 466, 946
Lai D., 1994, MNRAS, 270, 611
Lai D., Wiseman A. G., 1996, Phys. Rev. D, 54, 3958
Lai D., Wu Y., 2006, Phys. Rev. D, 74, 024007
Marsh T., Gaensicke B. T., Steeghs D., Southworth J., Koester D., Harris V., Merry L., 2010, preprint (arXiv:1002.4677)
Mullally F., Badenes C., Thompson S. E., Lupton R., 2009, ApJ, 707, L51
Nelemans G., 2009, Classical Quantum Gravity, 26, 094030
Nelemans G., Yungelson L. R., Portegies Zwart S. F., Verbunt F., 2001, A&A, 365, 491
Ogilvie G. I., Lin D. N. C., 2004, ApJ, 610, 477
Ogilvie G. I., Lin D. N. C., 2007, ApJ, 661, 1180
Peters P. C., 1964, Phys. Rev. B, 136, 1224
Press W. H., Teukolsky T. A., 1977, ApJ, 213, 183
Press W. H., Teukolsky S. A., Vetterling W. T., Flannery B. P.., 2007, Numerical Recipes. Cambridge Univ. Press, Cambridge
Racine E., Phinney E. S., Arras P., 2007, MNRAS, 380, 381
Ramsay G., Hakala P., Wu K., Cropper M., Mason K. O., Cordova F. A., Priedhorsky W., 2005, MNRAS, 357, 49
Rathore Y., Blandford R. D., Broderick A. E., 2005, MNRAS, 357, 834
Reisenegger A., 1994, ApJ, 432, 296
Reisenegger A., Goldreich P., 1994, ApJ, 426, 688
Shibata M., 1994, Prog. Theo. Phys., 91, 871
Steinfadt J., Kaplan D. L., Shporer A., Bildsten L., Howell S. B., 2010, ApJ, 716, L146
Strohmayer T. E., 2005, ApJ, 627, 920
Unno W., Osaki Y., Ando H., Saio H., Shibahashi H., 1989, Nonradial Oscillations of Stars. University of Tokyo Press, Japan
Willems B., Deloye C. J., Kalogera V., 2010, ApJ, 713, 239
Wu Y., 1998, PhD thesis, California Institute of Technology
Wu Y., 2005, ApJ, 635, 688
Wu Y., Goldreich P., 1999, ApJ, 519, 783
Zahn J. P., 1970, A&A, 4, 452
Zahn J. P., 1989, A&A, 220, 112
Zahn J.-P., 2008, Econometrics Applied Statistics Unit, 29, 67

This paper has been typeset from a TEX/LATEX file prepared by the author.